



HAL
open science

Impact of the TAP-like transporter in antigen presentation and phagosome maturation

Myriam Lawand, Irimi Evnouchidou, Thomas Baranek, Sebastian Montealegre, Sha Tao, Ingo Drexler, Loredana Saveanu, Mustapha Si-Tahar, Peter van Endert

► To cite this version:

Myriam Lawand, Irimi Evnouchidou, Thomas Baranek, Sebastian Montealegre, Sha Tao, et al.. Impact of the TAP-like transporter in antigen presentation and phagosome maturation. *Molecular Immunology*, 2019, 113, pp.75 - 86. 10.1016/j.molimm.2018.06.268 . hal-03534442

HAL Id: hal-03534442

<https://univ-tours.hal.science/hal-03534442>

Submitted on 20 Jul 2022

HAL is a multi-disciplinary open access archive for the deposit and dissemination of scientific research documents, whether they are published or not. The documents may come from teaching and research institutions in France or abroad, or from public or private research centers.

L'archive ouverte pluridisciplinaire **HAL**, est destinée au dépôt et à la diffusion de documents scientifiques de niveau recherche, publiés ou non, émanant des établissements d'enseignement et de recherche français ou étrangers, des laboratoires publics ou privés.



Distributed under a Creative Commons Attribution - NonCommercial 4.0 International License

Impact of the TAP-like transporter in antigen presentation and phagosome maturation

Myriam Lawand^a, Irini Evnouchidou^{a1}, Thomas Baranek^{b1}, Sebastian Montealegre^a, Sha Tao^c,
Ingo Drexler^c, Loredana Saveanu^a, Mustapha Si-Tahar^b, Peter van Endert^a

^a Institut National de la Santé et de la Recherche Médicale, Unité 1151; Université Paris Descartes, Faculté de médecine ; Centre National de la Recherche Scientifique, UMR8253 ; 149 rue de Sèvres, 75743 Paris Cedex 15, France

^b Institut National de la Santé et de la Recherche Médicale, Unité 1100 ; Université F. Rabelais, Faculté de médecine ; Centre d'études des pathologies respiratoires ; 10 Boulevard Tonnellé, 37032 Tours Cedex, France

^c Institut für Virologie, Universitätsklinikum Düsseldorf, Heinrich-Heine Universität, 40225 Düsseldorf, Germany

Corresponding author: peter.van-endert@inserm.fr

¹ These authors contributed equally

Abstract

Cross-presentation is thought to require transport of proteasome-generated peptides by the TAP transporters into MHC class I loading compartments for most antigens. However, a proteasome-dependent but TAP-independent pathway has also been described. Depletion of the pool of recycling cell surface MHC class I molecules available for loading with cross-presented peptides might partly or largely account for the critical role of TAP in cross-presentation of phagocytosed antigens. Here we examined a potential role of the homodimeric lysosomal TAP-like transporter in cross-presentation and in presentation of endogenous peptides by MHC class II molecules. We find that TAP-L is strongly recruited to dendritic cell phagosomes at a late stage, when internalized antigen and MHC class I molecules have been degraded or sorted away from phagosomes. Cross-presentation of a receptor-targeted antigen *in vitro* and of a phagocytosed antigen *in vivo*, as well as presentation of a cytosolic antigen by MHC class II molecules, is not affected by TAP-L deficiency. However, accumulation *in vitro* of a peptide optimally adapted to TAP-L selectivity in purified phagosomes is abolished by TAP-L deficiency. Unexpectedly, we find that TAP-L deficiency accelerates phagosome maturation, as reflected in increased Lamp2b recruitment and enhanced proteolytic degradation of phagocytosed antigen and *in vitro* transported peptides. Although additional experimentation will be required to definitely conclude on the role of TAP-L in transport of peptides presented by MHC class I and class II molecules, our data suggest that the principal role of TAP-L in dendritic cells may be related to regulation of phagosome maturation.

Keywords: transporter, peptide, cross-presentation, dendritic cell, MHC

1. Introduction

Presentation of exogenous antigens by the major histocompatibility complex class I (MHC-I) molecules, referred to as cross-presentation, allows dendritic cells (DCs) to initiate cytotoxic CD8⁺ T responses against pathogens and tumors as well as to induce tolerance to self-proteins [1]. Several intracellular pathways mediating cross-presentation have been described. Although definite evidence on the relative impact of the different pathways is missing, most authors assume that the dominant pathways require the heterodimeric transporters associated with antigen processing (TAP) [2]. In support of this concept, genetic invalidation of TAP compromises cross-presentation of the model antigen ovalbumin (OVA) internalized by DCs in various forms including OVA coated on latex beads, targeted to different DC surface receptors, or added as soluble protein [3]. It is thought that TAP can import peptide fragments derived by cytosolic degradation of internalized antigens produced either into the perinuclear endoplasmic reticulum (ER) or into phagosomes and/or endosomes having acquired TAP through Sec22b-mediated fusion with the ER [4]. In support of the latter, selective TAP inhibition in endosomes inhibited cross-presentation of receptor-targeted antigen [5, 6].

Interpretation of cross-presentation assays with TAP-deficient DCs is complicated by the fact that such cells express low numbers of MHC-I molecules on the surface due to quality control mechanisms that retain empty MHC-I in the ER [7]. Given that recycling of cell surface molecules is thought to be an important source for cross-presenting MHC-I molecules [8], it is conceivable that a dearth of such molecules contributes to the effect of TAP deficiency on cross-presentation. This consideration prompted our group previously to re-examine the role of TAP in cross-presentation, using an experimental setup that allowed to examine separately the role as transporter of cross-presented peptides and the role in providing cell surface class I molecules for recycling [9]. Using TAP-deficient cells expressing near-normal levels of cell surface MHC-I molecules following an overnight incubation at low temperature, we found

that reconstitution of surface MHC-I levels was sufficient to normalize cross-presentation of phagocytosed but not of a receptor-targeted OVA. Remarkably, reconstituted cross-presentation was proteasome-dependent, suggesting antigen degradation in the cytosol [9]. This raised the possibility of a TAP-independent mechanism allowing the transport of peptides from the cytosol into phagosomes. Consistent with this, we demonstrated recently that the OVA epitope SIINFEKL (S8L), recognized by OT-I T cells used in most studies of cross-presentation, can be imported in vitro into crude phagosomes in an ATP-dependent but TAP-independent manner, while phagosome accumulation of another epitope was strictly TAP-dependent [10].

In this study, we examined the possibility that the lysosomal transporter TAP-Like (TAP-L, also ABCB9) is responsible for TAP-independent import of S8L into phagosomes and consequently involved in cross-presentation. TAP-L is a homodimeric protein homologous to TAP that belongs to the family of ATP-binding cassette transporters [11]. In contrast to the ER-localized TAP complex, TAP-L is found in late endosomal or lysosomal compartments, where it co-localizes with, and is stabilized by physical interaction with, Lamp1 and Lamp2 [12]. TAP-L is thought to transport peptides from the cytosol into Lamp⁺ compartments [13], however a functional role has not been described so far [14]. TAP-L transports peptides with higher capacity but lower affinity than TAP and displays a broad peptide specificity, transporting 6- to 59-mers with a preference for 23-mers [15]. TAP-L is strongly up-regulated during GM-CSF-driven differentiation of human monocytes to “inflammatory” DCs [11]. Thus localization, specificity and regulation of TAP-L are compatible with a potential role in cross-presentation and MHC-II presentation of peptides produced in the cytosol [14], a hypothesis subjected to initial examination in this paper.

2. Material and Methods

2.1. Mice and cells

Production of TAP-L^{-/-} mice has been described previously [16]. TAP-L^{-/-} mice were crossed with TAP^{-/-} mice to obtain homozygous TAP/TAP-L double KO mice along with their C57/BL6 WT littermates. Bone marrow-derived DCs (BM-DCs) generated by incubation with GM-CSF were used on day 6 or 7 of differentiation for experiments, as described [10]. Where indicated, BM-DCs were pre-incubated overnight for 16 hrs at 26°C. For antigen presentation assays, lymph node cells from C57BL/6 RAG^{-/-} OT-I T cell receptor-transgenic mice, recognizing the peptide OVA₂₅₇₋₂₆₄ (S8L), were used as readout [17].

2.2. Cell phenotyping

Spleens and thymuses were subjected to red blood cell lysis and then labeled for 20 min at 4°C with 2 µg/ml of antibodies with the following specificities in FACS buffer (PBS with 0.5% bovine serum albumin): CD4 (clone RM4-5), CD8 (clone 53.6.7), CD19 (clone 6D5), NK1.1 (NKR-P1B and NKR-P1C), CD11b (clone M1/70) (all from BD Biosciences), T cell receptor β chain (clone H57-597), CD11c (clone N418) (ebioscience), MHC-II (clone M5/114.15.2) (Biolegend). After washing in FACS buffer the cells were analyzed on a FACSCanto machine (BD Biosciences). Data was processed using FlowJo software.

BM-DCs were stained with MHC class II, H2-L^d (Fig. 3) and H2-K^b (Fig. 4) antibodies: 64.3.7 (free H2-L^d heavy chains), 30.5.7 (H2-L^d /peptide complexes), AF6.88.5 (H2-K^b, conformational) and clone B8.24.3 (H2-K^b, non-conformational).

2.3. TAP-L-GFP cloning

E-GFP was amplified from pEGFP-N1 (Clontech) with the following primers:

5' TA GGA TCC GGC GGA AGC GGC GGA TCT *GTG AGC AAG GGC GAG GAG* 3'

(forward) and 5' TA GGTACC TTA CTT GTA CAG CTC GTC CA 3' (reverse) and cloned in pcDNA3.1-hygro between the BamHI and KpnI sites, generating plasmid pcDNA3.1-

hygro-EGFP. Human TAP-L was amplified from HeLa cDNA with the following primers: 5' TA GCT AGC ACC ATG CCG CTG TGG AAG GCG GT 3' (forward) and 5' TA GGATCC TCC GGC CTT GTG ACT GCC GTT GG 3' (reverse). The PCR product was cloned in pcDNA3.1-hygro-EGFP between the NheI and BamHI sites, generating plasmid pCDNA/TAP-L-GFP. For inducible expression, the TAP-L cDNA was fused to a carboxyterminal hemagglutinin tag cloned in the doxycyclin-inducible plasmid pTRETight (Clontech), as described previously [18], generating plasmid pTRETight/TAP-L-HA.

2.4. Microscopy

HeLa tet-on cells were transfected by electroporation with pTRETight/TAP-L-HA, using described conditions [18], followed by induction of TAP-L expression by addition of 100 ng/ml doxycycline 24hrs later. BM-DCs (2×10^6) were transfected on day 6 with 2 μ g of pCDNA/TAP-L-GFP using an AMAXA kit (Lonza, Germany). Transfected HeLa cells and BM-DCs were seeded on fibronectin coated slides 24hrs or 36hrs later, respectively, fixed with 4% paraformaldehyde, permeabilized with saponine 0.2%, BSA 0.2% in PBS, and stained for analysis by confocal microscopy. HeLa cells were stained with rat anti-HA tag (Roche, clone 3F10), mouse anti-human EEA1-FITC (BD Biosciences, clone 14) and mouse anti-human Lamp1-FITC (BD Biosciences, clone H4A3) monoclonal antibodies (mAbs). BM-DCs were stained with a rat anti-Lamp1 mAb (BD Biosciences, clone 1D4B) and polyclonal rabbit antibodies against syntaxin 6 (Proteintech), insulin-regulated aminopeptidase (IRAP; a gift from S. Keller) and Rab14 (Sigma Aldrich). To monitor TAP-L localization during phagocytosis, pCDNA/TAP-L-GFP transfected BM-DCs were seeded in IBIDI™ (Biovalley) slides and fed with yeast expressing OVA [19] for 10, 20 or 60 min. Cells were fixed and permeabilized as described above and stained with rat anti-Lamp1 (clone 1D4B) and rabbit polyclonal antibodies against OVA (Sigma-Aldrich). For the staining of cell surface MHC-I, cells were incubated before phagocytosis with B22 antibody at 4°C for

15 min. Images were acquired on a Leica DMI 6000 microscope equipped with a piezoelectric-driven stage and Optophotonics XF202 (FITC narrow) and XF102-2 (Texas Red) filters. Images were deconvoluted using Metamorph™ 6.3.7. The percentage of TAP-L co-localizing with other markers was calculated using Image J software. The percentage of co-localization is reported as the proportion of fluorescence of marker one overlaying with marker two. MHC class I and class II staining of TAP-L-GFP transfected steady-state BM-DCs was analyzed using a Leica SP8 confocal microscope.

2.5. *In vitro* cross-presentation of OVA

Complexes between the fusion protein P3UOVA [20] and CD11c antibodies (clone N418) were formed by a 30min incubation at 4°C of equimolar amounts of the two components. CD11c-targeted complexes (6 µg/ml, 2 µg/ml and 0.7 µg/ml) were then added for 4hrs at 37°C to BM-DCs pre-incubated at 37°C or 26°C. Then BM-DCs were fixed and incubated with OT-I cells at a ratio 1:1 for 24hrs at 37°C. The IL-2 concentration in supernatants was analyzed by sandwich ELISA, as described [9].

2.6. MHC class II presentation assay

BM-DCs and antigen-specific CD4⁺ T cell lines were generated as earlier described [21]. Briefly, BM-DCs were infected with either modified vaccinia Ankara (MVA) or vaccinia virus (VACV) at an MOI 1 or 10 for 7h at 37°C. Additionally, uninfected BM-DCs were plated at the same density and pulsed with ova peptide (2µg/ml) as positive or negative controls, respectively. 1×10^5 infected BM-DCs were plated in 96-well F-bottom plates and 3×10^5 OVA-specific-CD4⁺ T cells were added per well (effector:target ratio 2:1) in the presence of 1µg/ml brefeldin A. After incubation for 14h at 37°C, the cells were transferred into V-bottom 96-well plates and incubated with blocking buffer (PBS + 1% BSA + 1µg/ml ethidium monoazide bromide) for 20min under light exposure to exclude dead cells.

Thereafter, intracellular cytokine staining of CD4⁺ T cells for IFN-γ was performed using the

BD Cytotfix/Cytoperm™ Fixation / Permeabilization Kit following the manufacturer's protocol (BD Pharmingen™, Heidelberg, Germany). Briefly, cells were washed twice with blocking buffer and surface staining was performed with CD4 antibodies for 30min at 4°C. Cells were washed and permeabilization was performed with Cytotfix/Cytoperm™ Solution for 15min at 4°C. Thereafter, cells were washed again and incubated with anti-IFN-γ for 30min at 4°C. Flow cytometric analysis of cells fixed with 1% PFA was performed on a BD FACSCanto II equipment (BD Biosciences, Heidelberg, Germany). Anti-Mouse CD4 eFluor®450 and Anti-Mouse IL2 APC were purchased from eBioscience (Frankfurt, Germany). Rat Anti-Mouse IFN-γ FITC was from BD Pharmingen™ (Heidelberg, Germany). Antigen-specific peptides (B5R₄₆₋₆₀, OVA₂₆₅₋₂₈₀) were produced by Biosyntan GmbH (Berlin, Germany).

2.7. *In vivo* cross-presentation of OVA

Lymph node cells from OT-I mice cells were labeled with 5μM CellTrace™ Cell Proliferation Kit (Life Technologies) for 10min at 37°C in PBS with 0.1% BSA, washed, resuspended in PBS with 0.5% BSA and injected intravenously at 1x10⁶/100μl. The next day, 4 x 10⁶ splenocytes from Balb/c mice depleted of red blood cells were electroporated with 1.5 mg/ml OVA protein using a GenePulser Xcell electroporator (Biorad) at 300V and 500μF. The electroporated and washed cells were exposed to ultraviolet radiation at 2 x 10⁵ μJoule (UV-Stratalinker, Stratagene), resuspended in PBS with 0.5% BSA and injected i.v. at 1x10⁶ in 100μl. BM-DCs loaded with 10⁻⁷M S8L peptide were injected as a positive control to WT mice. After another 3 days, the splenocytes of the injected mice were recovered, labeled with mAbs against CD8 (clone 53.6.7) and Vβ5.1-5.2 (clone MR9-4) (BD Biosciences) at 5 μg/ml for analysis of CFSE dilution by flow cytometry.

2.8. Mouse infection

TAP-L^{-/-} and TAP-L^{+/+} littermates aged between 8 and 12 weeks were anesthetized by intraperitoneal injection of ketamine (50 mg/kg) and xylazine (10 mg/kg) and challenged intranasally with 150 pfu (DL50) or 300 pfu (lethal dose) of influenza/A/Scotland/20/74 (H3N2) viral stocks prepared as described previously [22]. The mice were monitored every day for weight, signs of illness and mortality for up to 15 days. All experiments were performed in the animal facilities of Tours University according to guidelines of the local ethical committee.

2.9. Analysis of phagosomal OVA degradation

BM-DCs were incubated with 3 µm polybeads coated with 0.5 mg/mL OVA for 20 and 120 min to allow for formation early and late phagosomes, respectively, before lysis for 1hr at 4°C in a buffer containing 50mM Tris pH 7.4, 150mM NaCl, 0.5% NP40, 1mM DTT, 10µg/ml DNase I. The beads were recovered by centrifugation at 2,650×g and a series of washes for 3min at 4°C, stained with rabbit anti-OVA antibodies (5µg/ml) followed by AlexaFluor 488-conjugated anti-rabbit antibodies (Invitrogen, 5µg/ml) and analyzed by flow cytometry.

2.10. Phagosomal maturation and peptide transport assays

Three µm immunoglobulin (Ig)-coated polybeads, or streptavidin-coupled beads were used to prepare crude phagosomes as previously described [10]. To analyze phagosome maturation, BM-DCs were stimulated with 100 ng/ml LPS (E.coli, 055:B5; Sigma Aldrich) for 100min before and during phagocytosis of Ig-coupled beads. Then the phagosomes were purified and stained with anti-Lamp-2b antibody, as described [10]. Accumulation of the FITC-conjugated peptides RRYNACTEL (R9L-FITC) and S8L-FITC in phagosomes containing Ig-coated beads was analyzed exactly as described previously [10]. Here we also used the 23-mer peptide FVALREIRRYNAC(FITC)TELLIRK(Biotin)LPR (F23R(Bio)-FITC) (>95% purity, Biosyntan, Germany) designed according to the specificity of TAP-L [15].

F23R(Bio)-FITC was added at various concentrations to phagosomes containing streptavidin-coated beads. Where indicated, transport assays with F23R(Bio)-FITC were performed in the presence of EDTA-free cOmplete protease inhibitors (Roche Diagnostics, Meylan, France). To monitor accumulation of R9L-FITC and S8L-FITC, complete phagosomes were analyzed, while phagosomes with F23R(Bio)-FITC were lysed using PBS with 1% BSA and 1% SDS before analysis of beads by flow cytometry.

2.11. Statistical analysis

All results are expressed as means \pm SEM. Statistical significance was determined using the Mantel-Cox test for survival curves. Data were analyzed using GraphPad Prism 5 (GraphPad Software). p-values <0.05 were considered significant.

3. Results

3.1. Immune phenotype of TAP-L^{-/-} mice

To determine whether TAP-L deficiency affected the gross development of the immune system, we examined the proportions of key immune cells in the thymus and the spleen. TAP deficient mice harbored reduced numbers of single-positive CD8⁺ thymocytes, consistent with published data [7]. In contrast, absence of TAP-L had no effect on thymocyte proportions and did not reduce further the proportion of CD8⁺ thymocytes present in TAP^{-/-} mice (Fig. 1A). Similarly, TAP-L knockout alone did not modify the proportion of splenic CD8⁺ or CD4⁺ splenocytes present in WT or TAP^{-/-} mice (Fig. 1B, C). TAP-L^{-/-} mice harbored normal proportions of CD11b⁺CD8⁻ and CD11b⁻CD8⁺ conventional DCs (cDC1 and cDC2) in the spleen (Fig. 1D). The percentages of B, NK and NK-T cells were also identical between the four types of mice analyzed (data not shown).

Next we examined the potential effect of TAP-L knockout on expression of MHC-I molecules. While TAP deficiency decreased class I expression by > 50% at physiologic temperature, TAP-L knockout did not affect expression of molecules recognized by the conformational mAb AF6.88 and the non-conformational mAb B8.24.3 (Fig. 2). Overnight incubation of BM-DCs at low temperature not only increased expression of MHC-I molecules (as detected by the non-conformational mAb B8.24.3) by TAP^{-/-} cells, but also by WT cells, both observations being consistent with the literature [9, 23, 24]. TAP-L deficiency had no effect on expression of MHC-I molecules at 37°C and also did not affect the increase following incubation at 26°C of WT and of TAP^{-/-} cells (Fig. 2). Thus TAP-L is not required for thymic selection and peripheral survival of T cells, normal abundance of splenic cDC1 and cDC2, and physiologic expression of MHC-I and MHC-II molecules by splenocytes. We also concluded that TAP-L is not responsible for the reconstitution of MHC class I expression on the cell surface upon cell incubation at 26°C.

3.2. Intracellular localization of TAP-L

To determine the intracellular localization of TAP-L, we expressed TAP-L in fusion with GFP or an HA-tag in BM-DCs and HeLa cells, respectively. In steady state conditions, TAP-L co-localized with the lysosomal marker Lamp1, in both cell types. Additional staining for endocytic compartments showed that TAP-L co-localized neither with IRAP and Rab14, both marking DC early endosomes [25], nor with the trans-Golgi and endosomal protein syntaxin 6 (Fig. 3A, C; see Fig. S1 and S2 for separate green and red channels of Fig. 3 images). In BM-DCs, a minor part of TAP-L (20%) co-localized with “open” and fully conformed MHC-I molecules; this pool of MHC-I molecules corresponded to < 5% of the cellular total, presumably because of substantial presence on the surface where no TAP-L is found (Fig. 3B). In HeLa cells, this percentage was even lower, with < 10% of TAP-L co-localizing with MHC-I, EEA-1 and IRAP (Fig. 3C). Conversely, on average >50% of cellular TAP-L co-localized with MHC-II, with a range from 30% to 80% corresponding to different activation states and MHC-II distribution between the surface and the interior of the BM-DCs (Fig. 3B). These results are consistent with the lysosomal localization of TAP-L reported previously [26] but demonstrate the partial presence of TAP-L in MHC-I loading compartments in steady state conditions.

To investigate TAP-L localization during phagocytosis, we fed BM-DCs with yeast cells decorated with OVA [19] and analyzed them at different time points by confocal microscopy. Like in steady-state conditions, TAP-L strongly co-localizes with Lamp1 during phagocytosis and, starting from 20 min after yeast up-take, TAP-L and Lamp1 are both recruited to the phagosomal membrane (Fig. 4A, D; see Fig. S3 for separate red/green channels of Fig. 4 images). TAP-L-GFP showed very limited co-localization with internalized MHC-I molecules (Fig. 4B, D) and with OVA decorating internalized yeasts (Fig. 4C, D). Internalized MHC-I (Fig. 4B) and OVA (Fig. 4C) staining was maximal at early time points of phagocytosis and

decreased with phagosomal maturation, whereas the amount of phagosomal TAP-L and Lamp1 increased at the same time (Figure 4D). The relatively fast disappearance of OVA staining in this experiment may be due to activation of pattern recognition receptors by yeast that can accelerate phagosome maturation. Thus, TAP-L is recruited strongly to phagosomes, however mainly at a time point when internalized MHC-I molecules and OVA cannot be detected any more.

3.3. Cross-presentation by TAP-L^{-/-} BM-DCs and mice

Our starting hypothesis was that TAP-L might be responsible for TAP-independent import of peptide S8L into phagosomes [10] involved in reconstitution of cross-presentation of phagocytosed antigen by DC pre-incubation at 26°C [9]. To test this, we examined cross-presentation of different OVA forms *in vitro* and *in vivo*. Pulsing with a soluble OVA fusion protein targeted to CD11c [20] resulted in dose-dependent cross-presentation of S8L by WT BM-DCs and was not affected by DC pre-incubation at 26°C (Fig. 5A). TAP^{-/-} BM-DCs pre-incubated at 37° or 26°C were unable to cross-present receptor-targeted OVA, consistent with the obligatory requirement of TAP for cross-presentation of antigen internalized in this way described previously by us [9, 20]. In contrast, TAP-L knockout had no discernable effect on cross-presentation of CD11c-targeted OVA (Fig. 5A). Next we examined cross-presentation of a phagocytosed antigen *in vivo*. Mice were injected with OT-I T cells and MHC-disparate splenocytes electroporated with OVA, and proliferation of OT-I cells, as reflected by CFSE dilution, was examined by flow cytometry. Both WT and TAP-L^{-/-} mice showed vigorous OT-I proliferation, equivalent to that induced by peptide-pulsed BM-DCs injected in WT mice, whereas TAP deficiency abolished T cell proliferation almost entirely (Fig. 5B). We concluded that TAP-L is not required for cross-presentation of phagocytosed OVA *in vivo*.

Given the localization of TAP-L in Lamp⁺ compartments and its strong co-localization with MHC-II molecules, it was conceivable that TAP-L acts as a transporter for peptides produced

in the cytosol and loaded on MHC-II molecules. We addressed this possibility using a previously described system in which vaccinia or MVA virus-infected cells present cytosolic OVA to specific CD4⁺ T cells [21]. In this system, OVA presentation depends on antigen neosynthesis and is inhibited (though not completely) by epoxomicin but not by TAP deficiency [21], so that a role of the proteasome in epitope production is likely, and a role for TAP-L in peptide transport conceivable. As shown in Fig. 5C, CD4⁺ T cells responded to infected BM-DCs in a virus dose-dependent and specific manner, however without any effect of TAP-L deficiency. Thus at least in this system, TAP-L does not transport peptides into an MHC-II loading compartment.

3.4. Role of TAP-L in peptide accumulation in BM-DC phagosomes

Considering that TAP-L can transport peptides of various lengths including that required for MHC-I presentation, and that TAP-L is recruited strongly to BM-DC phagosomes, we asked whether a role of TAP-L in peptide import into phagosomes can be detected in vitro. To address this, we used the phagoFACS assay previously adopted by us to measure ATP-dependent accumulation of FITC-labeled reporter peptides in crude phagosomes [10]. Initially we tested two peptides with a length adapted to MHC-I binding: R9L-FITC, a peptide with high affinity for the TAP transporter [27], and S8L-FITC with intermediate affinity for TAP [28]. Consistent with our previous observations, accumulation of peptide R9L was TAP-dependent, while peptide S8L accumulated also in TAP-deficient phagosomes (Fig. 6A). In contrast, deficiency for TAP-L alone or in combination with TAP reduced accumulation of S8L by about 60% but had no effect on R9L. Therefore different peptides may display distinct dependence on phagosomal peptide transporters.

Unlike TAP, which selects peptides of 8 to 16 residues [29], TAP-L prefers longer peptides, with an optimal length of 23 residues [15]. We examined the role of TAP-L in transport of a

23-mer peptide using a modified phagoFACS assay, in which the both FITC- and biotin-labeled peptide could bind to streptavidin-coated beads. This assay provides direct evidence for peptide import into the lumen of phagosomes rather than association with it. Incubation of WT phagosomes with the peptide F23R(Bio)-FITC resulted in substantial peptide accumulation within phagosomes, which was completely abolished by TAP-L deficiency (Fig. 6B). TAP deficiency had no effect on F23R(Bio)-FITC import (not shown). Note that accumulation of the 23-mer required incubation with at least 150 nM peptide, a relatively high concentration considering our previous observation that TAP-dependent accumulation of R9L(Bio)-FITC requires only 2 nM peptide [10]. TAP-L has been shown to bind peptides with lower affinity than TAP [15], consistent with this result. We concluded that TAP-L can import long and possibly also some short peptides into phagosomes.

3.5 TAP-L deficiency enhances susceptibility to influenza virus infection

The strong co-localization of TAP-L with Lamp1/2 suggests that TAP-L is present in MHC-II loading compartments. The published preference of TAP-L for longer peptides, together with our demonstration of transport of a 23-mer into phagosomes (Fig. 6), suggest that TAP-L might provide peptides derived by cytosolic degradation of endogenous proteins, into MHC-II loading compartments. Presentation of TAP-independent but proteasome-dependent peptides by MHC-II molecules to CD4⁺ T cells has recently been reported to occur during influenza infection [30]. To obtain initial evidence for a potential role of TAP-L in T cell responses to influenza virus, we examined the survival of TAP-L^{-/-} mice upon infection with influenza A virus (IAV). Interestingly, TAP-L^{-/-} mice infected with 300 pfu of IAV (lethal dose) died earlier (10 to 12 days) compared to their littermate controls (11 to 15 days) (Fig. 7B). However this difference was not found at lower doses (100 pfu and 150 pfu) (data not shown and Fig 7A).

3.6 Degradation of OVA and peptide F23R(Bio)-FITC in TAP-L^{-/-} phagosomes

Maturation of phagosomes is a highly regulated process ultimately producing an acidic degradative compartment, which in DCs is tuned in order to avoid premature complete degradation of internalized protein and peptide antigens. To assess whether TAP-L deficiency affects phagosome maturation, we examined degradation of OVA coated on latex beads. While WT and TAP-L^{-/-} early phagosomes contained equivalent amounts of OVA, late TAP-L^{-/-} vesicles contained much less OVA than control vesicles (Fig. 8A), suggesting enhanced proteolytic activity in late phagosomes. Consistent with this, late TAP-L^{-/-} phagosomes stained more strongly for Lamp2b (Fig. 8B). Considering that stronger proteolytic activity may also degrade peptides imported into phagosomes, we examined accumulation of the peptide F23R(Bio)-FITC in the presence of protease inhibitors. Protease inhibition reconstituted accumulation of peptide in TAP-L^{-/-} phagosomes completely (150 nM) or partly (300 and 600 nM) but had no effect in WT phagosomes (Fig. 8C), suggesting that the effect of TAP-L deficiency on peptide accumulation is at least partly due to enhanced peptide degradation.

4. Discussion

We report an initial characterization of mice and DCs lacking TAP-L, a transporter with a potential involvement both in cross-presentation and in presentation of endogenous peptides by MHC-II molecules. TAP-L^{-/-} mice display normal development and abundance of the principal thymic and splenic immune cells as well as normal expression of MHC-I and MHC-II molecules, ruling out a key function in antigen presentation.

Localization of TAP-L in Lamp⁺ vesicles of HeLa cells and BM-DCs was expected, given previous results obtained with human cells [14]. This positions TAP-L as a potential mechanism for importing peptides produced in the cytosol for loading on MHC-II molecules. Apparently proteasome-produced but TAP-independent MHC-II presented epitopes have been described by several investigators [21, 30]. However, studying VACV-infected BM-DCs presenting an at least partly proteasome-dependent epitope, we do not find evidence for such a role of TAP-L. With respect to our main objective of exploring a potential role of TAP-L in cross-presentation of phagocytosed antigens, the subcellular localization of TAP-L upon phagocytosis provides some indication. It is clear that TAP-L is mainly recruited to late phagosomes having lost detectable OVA and MHC-I molecules (Fig. 4). Although most authors including we assume that cross-presenting MHC-I molecules are loaded in early endocytic vesicles [6, 25, 31], some authors attributed loading to Lamp⁺ vesicles [32, 33]. Absent co-localization between TAP-L and phagocytosed OVA does not argue strongly against a role for TAP-L in cross-presentation, since antigenic peptides may be present when OVA is degraded. However, the low level of co-localization between TAP-L and MHC-I during phagosome maturation argues against a role of TAP-L in cross-presentation. While OVA seemed completely degraded 2 hrs after phagocytosis, MHC-I molecules seemed to segregate into small endocytic vesicles devoid of TAP-L at this time, i.e. to be sorted away from phagosomes before arrival of TAP-L.

Direct examination of TAP^{-/-} BM-DCs and mice did not uncover any evidence for a role of TAP-L in cross-presentation. Lack of TAP-L implication was expected in the case of receptor-targeted antigen. Although the presumably distinct [9] vesicular environments involved in cross-presentation of receptor-targeted antigens versus phagocytosed antigens remain to be determined, their complete TAP dependence renders an ER-type environment likely and thus a role of TAP-L unlikely for the former. Our hypothesis had been that TAP-L might play a role in TAP-independent cross-presentation of phagocytosed antigens. Cross-presentation of OVA-transfected splenocytes *in vivo* was not affected by TAP-L; however, since this experimental system was almost completely TAP-dependent, answering our hypothesis will require setting up experimental systems suited better to the issue under investigation.

Phagosomal peptide transport assays provided at first sight evidence in support of a role of TAP-L in importing a 23-mer and also S8L into phagosomes. This evidence was strongest for the peptide F23R(Bio)-FITC with a sequence designed for efficient TAP-L transport. However, monitoring degradation of OVA and acquisition of Lamp2b indicated altered maturation and enhanced proteolysis in TAP-L^{-/-} phagosomes. A phagosomal transport assay in the presence of protease inhibitors confirmed that this effect of TAP-L deficiency was at least partly responsible for the lack of 23-mer accumulation in TAP-L^{-/-} phagosomes. Although transport of relatively high concentrations of the 23-mer by TAP-L into late phagosomes is consistent with the subcellular localization of TAP-L as well as the peptide specificity and the affinity of TAP-L, it is impossible to determine the relative impact of TAP-L as peptide transporter and as modulator of phagosome maturation in the phenotype of TAP-L^{-/-} phagosomes. This uncertainty applies also to the effect of TAP-L knockout on resistance to influenza virus infection.

To conclude, our preliminary characterization indicates an unexpected role of TAP-L as modulator of phagosome maturation and a likely role as transporter of long peptides in late phagosomes, but does not provide evidence for a role of TAP-L in cross-presentation or MHC class II presentation of cytosolic antigens. Although additional experimental systems may be required to definitely conclude on the role of TAP-L in antigen presentation, the apparent absence of such a role is somewhat surprising. Indeed, the partial overlap between TAP-L and MHC-I presence in phagosomes, its significant co-localization with MHC-II, and the demonstration of TAP-L-mediated transport of S8L and the F23R in the phagoFACS assay all suggest that TAP-L should be able to pump cytosolic peptides into MHC loading compartments. Why then does this not occur? Since TAP-L colocalization with both MHC classes is partial, it is of course possible that MHC loading occurs in vesicles devoid of TAP-L. Another, and in our view more likely possible explanation is that the concentration of free peptides in the cytosol is so low and/or their half-life so short, that the low peptide affinity of TAP-L (contrasting with the higher affinity of TAP) is insufficient to extract significant amounts of peptides from the cytosol and provide them to MHC molecules.

Acknowledgements:

This work was supported by institutional grants from INSERM and Université Paris Descartes, by grants from the *Agence Nationale de Recherche* (10-PPPP-1236 and 14-CE11-0014) and the *Fondation pour la Recherche Médicale* (DEQ20130326539).

Figure Legends:

Figure 1. Immune cell populations in TAP-L KO mice. Percentages of CD4⁺ and CD8⁺ T cells in the thymus (A) and the spleen (B-C) of WT, TAP KO, TAP-L KO and TAP/TAP-L double KO mice were determined by flow cytometry. (D) Percentages of splenic CD11c^{hi}CD11b⁺CD8⁻ and CD11c^{hi}CD11b⁻CD8⁺ DCs and expression of MHC-II molecules in WT and TAP-L KO mice. The results are representative of 3 independent experiments.

Figure 2. Expression of MHC-I molecules. WT, TAP KO, TAP-L KO and double KO BM-DCs were pre-incubated at 26°C or 37°C before flow cytometric analysis of MHC-I expression using conformational (AF6.88.5.3) and non-conformational (B8.24.3) MHC-I mAbs. Unlabelled cells are used as negative control. The geometric mean of fluorescence is represented in the table. The results are representative of 3 independent experiments.

Figure 3. Localization of TAP-L in steady-state conditions

(A, B) BM-DCs from C57BL/6 (A) and Balb/c (B) mice were nucleofected with a plasmid encoding GFP-tagged TAP-L. Thirty-six hours later, the cells were stained with antibodies for LAMP1, Stx6, IRAP and Rab14 (A). In (B), cells were stained with antibodies recognizing free H2-L^d heavy chains (mAb 64.3.7), peptide-loaded H2-L^d molecules (mAb 30.5.7) and MHC class II molecules. Co-localization of TAP-L with the markers was analyzed for 5 cells from two independent experiments. (C) HeLa cells were transfected with a doxycyclin-inducible plasmid encoding HA-tagged TAP-L. Twenty-four hours after doxycyclin addition, the cells (n=6) were analyzed for TAP-L (i.e. HA) co-localization with EEA1 and Lamp1, as in (A).

Figure 4. TAP-L recruitment to phagosomes. BM-DCs were fed OVA-decorated yeast for 10, 20 or 60 min. Fixed and permeabilized cells were stained with antibodies against: Lamp1 (A) and OVA (B). For cell surface MHC-I visualization (C), cells were incubated before phagocytosis with B22 antibody at 4°C for 15 min and washed. Five cells each were quantified from two independent experiments and represented as the mean +/- SEM (D) at 10, 20 and 60min. Student t test was used for statistical analysis.

Figure 5. Cross-presentation and MHC class II presentation by TAP-L KO DCs. In (A), BM-DCs pre-incubated at 37°C or 26°C were incubated for 4hrs with CD11c-targeted OVA fusion protein and then cultured at a ratio 1:1 with OT-I cells for 24h. The production of IL-2 was analyzed by ELISA. The results are representative of 3 independent experiments. (B) Cross-presentation of apoptotic cells *in vivo*. Mice were injected *i.v.* with CFSE-labeled OT-I cells and one day later with irradiated H-2K^d splenocytes electroporated with soluble OVA. Another 3 days later, splenocytes were isolated and CFSE dilution in the CD8⁺Vβ5.1-5.2⁺ population was analyzed by flow cytometry. WT mice injected with SIINFEKL-pulsed BM-DCs were used as positive control. The results are representative of 3 independent experiments with 2 mice per group each. (C) BM-DCs prepared from TAP-L^{-/-} or WT C57BL/6 mice were infected with MVA or VACV at MOI 1 or 10 for 7h at 37°C, or pulsed with 2μg/mL OVA or control B5 peptide. Then OVA-specific-CD4⁺ T cells were added for 14h and intracellular IFN-γ accumulation was analyzed by flow cytometry. The results were calculated from 2 pooled independent experiments each with 3 mice/group.

Figure 6. Effect of TAP-L deficiency on peptide accumulation in phagosomes. (A). Crude phagosomes were prepared from BM-DCs pulsed with 3 μm latex beads and incubated with FITC-conjugated peptides R9L (left panels) or S8L (right panels). The accumulation of

fluorescent peptide in membrane-associated (CellMask⁺) phagosomes was analyzed by flow cytometry. (B) WT and TAP-L KO phagosomes containing streptavidin-coated beads were incubated with different concentrations of peptide F23R(Bio)-FITC. Then membranes were removed by SDS treatment and binding of FITC-labeled peptide to the beads was analyzed by flow cytometry. The results in (A) and (B) are representative of 3 independent experiments.

Figure 7. TAP-L deficiency enhances susceptibility to influenza virus infection. TAP-L^{-/-} mice (black boxes) and littermate TAP-L^{+/+} mice (grey circles) were infected *i.n.* with (A) 150 pfu or (B) 300 pfu of influenza/A virus. Statistical analysis was performed using the Mantel-Cox test (*: $p < 0.05$). The surviving mice were kept until day 20 post-infection.

Figure 8. (A) Degradation of OVA protein in WT and TAP-L KO phagosomes. BM-DCs were allowed to phagocytose OVA-coated latex beads for 20 and 120 min. After cell lysis by NP-40, OVA on beads was stained with rabbit polyclonal antibodies and quantified by flow cytometry. OVA beads isolated from phagosomes stained with the secondary antibody was the negative control, and non-phagocytosed OVA beads were the positive control. (B) Phagosomes from WT and TAP-L KO BM-DCs stimulated or not with LPS for 100 min were stained for Lamp2b. The results in (A) and (B) represent 3 and 2 independent experiments, respectively. (C) Accumulation of peptide F23R(Bio)-FITC was measured in the presence of a cocktail of protease inhibitors.

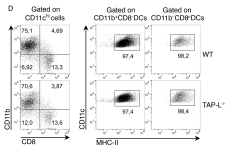
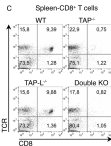
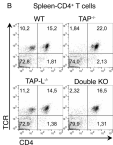
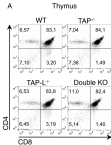
References

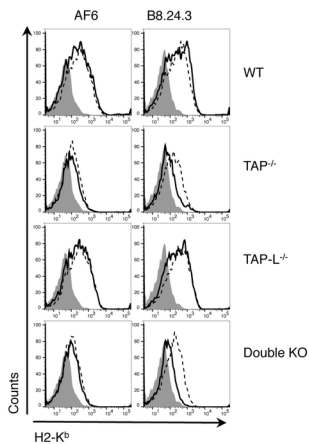
- [1] C. Kurts, B.W. Robinson, P.A. Knolle, Cross-priming in health and disease, *Nat Rev Immunol*, 10 (2010) 403-414.
- [2] S. Amigorena, A. Savina, Intracellular mechanisms of antigen cross presentation in dendritic cells, *Curr Opin Immunol*, 22 (2010) 109-117.
- [3] F.M. Cruz, J.D. Colbert, E. Merino, B.A. Kriegsmann, K.L. Rock, The Biology and Underlying Mechanisms of Cross-Presentation of Exogenous Antigens on MHC-I Molecules, *Annu Rev Immunol*, 35 (2017) 149-176.
- [4] I. Cebrian, G. Visentin, N. Blanchard, M. Jouve, A. Bobard, C. Moita, J. Enninga, L.F. Moita, S. Amigorena, A. Savina, Sec22b regulates phagosomal maturation and antigen crosspresentation by dendritic cells, *Cell*, 147 (2011) 1355-1368.
- [5] S. Burgdorf, A. Kautz, V. Bohnert, P.A. Knolle, C. Kurts, Distinct pathways of antigen uptake and intracellular routing in CD4 and CD8 T cell activation, *Science*, 316 (2007) 612-616.
- [6] S. Burgdorf, C. Scholz, A. Kautz, R. Tampe, C. Kurts, Spatial and mechanistic separation of cross-presentation and endogenous antigen presentation, *Nat Immunol*, 9 (2008) 558-566.
- [7] L. Van Kaer, P.G. Ashton-Rickardt, H.L. Ploegh, S. Tonegawa, TAP1 mutant mice are deficient in antigen presentation, surface class I molecules, and CD4-8+ T cells, *Cell*, 71 (1992) 1205-1214.
- [8] P. van Endert, Intracellular recycling and cross-presentation by MHC class I molecules, *Immunol Rev*, 272 (2016) 80-96.
- [9] N. Merzougui, R. Kratzer, L. Saveanu, P. van Endert, A proteasome-dependent, TAP-independent pathway for cross-presentation of phagocytosed antigen, *EMBO reports*, 12 (2011) 1257-1264.

- [10] M. Lawand, A. Abramova, V. Manceau, S. Springer, P. van Endert, TAP-Dependent and -Independent Peptide Import into Dendritic Cell Phagosomes, *J Immunol*, 197 (2016) 3454-3463.
- [11] O. Demirel, Z. Waibler, U. Kalinke, F. Grunebach, S. Appel, P. Brossart, A. Hasilik, R. Tampe, R. Abele, Identification of a lysosomal peptide transport system induced during dendritic cell development, *J Biol Chem*, 282 (2007) 37836-37843.
- [12] O. Demirel, I. Jan, D. Wolters, J. Blanz, P. Saftig, R. Tampe, R. Abele, The lysosomal polypeptide transporter TAPL is stabilized by interaction with LAMP-1 and LAMP-2, *J Cell Sci*, 125 (2012) 4230-4240.
- [13] C. Zhao, W. Haase, R. Tampe, R. Abele, Peptide specificity and lipid activation of the lysosomal transport complex ABCB9 (TAPL), *J Biol Chem*, 283 (2008) 17083-17091.
- [14] I. Bangert, F. Tumulka, R. Abele, The lysosomal polypeptide transporter TAPL: more than a housekeeping factor?, *Biological chemistry*, 392 (2011) 61-66.
- [15] J.C. Wolters, R. Abele, R. Tampe, Selective and ATP-dependent translocation of peptides by the homodimeric ATP binding cassette transporter TAP-like (ABCB9), *J Biol Chem*, 280 (2005) 23631-23636.
- [16] P. van Endert, M. Lawand, Unexpected lack of specificity of a rabbit polyclonal TAP-L (ABCB9) antibody, *F1000Res*, 4 (2015) 125.
- [17] K.A. Hogquist, S.C. Jameson, W.R. Heath, J.L. Howard, M.J. Bevan, F.R. Carbone, T cell receptor antagonist peptides induce positive selection, *Cell*, 76 (1994) 17-27.
- [18] H.T. Hsu, L. Janssen, M. Lawand, J. Kim, A. Perez-Arroyo, S. Culina, A. Gdoura, A. Burgevin, D. Cumenal, Y. Fourneau, A. Moser, R. Kratzer, F.S. Wong, S. Springer, P. van Endert, Endoplasmic reticulum targeting alters regulation of expression and antigen presentation of proinsulin, *J Immunol*, 192 (2014) 4957-4966.

- [19] L. Saveanu, P. van Endert, Preparing antigens suitable for cross-presentation assays in vitro and in vivo, *Methods Mol Biol*, 960 (2013) 389-400.
- [20] R. Kratzer, F.X. Mauvais, A. Burgevin, E. Barilleau, P. van Endert, Fusion proteins for versatile antigen targeting to cell surface receptors reveal differential capacity to prime immune responses, *J Immunol*, 184 (2010) 6855-6864.
- [21] F. Thiele, S. Tao, Y. Zhang, A. Muschwackh, T. Zollmann, U. Protzer, R. Abele, I. Drexler. Modified vaccinia virus Ankara-infected dendritic cells present CD4+ T-cell epitopes by endogenous major histocompatibility complex class II presentation pathways, *J Virol*, 89 (2015) 2698-2709.
- [22] L. Guillot, R. Le Goffic, S. Bloch, N. Escriou, S. Akira, M. Chignard, M. Si-Tahar, Involvement of toll-like receptor 3 in the immune response of lung epithelial cells to double-stranded RNA and influenza A virus, *J Biol Chem*, 280 (2005) 5571-5580.
- [23] H.G. Ljunggren, N.J. Stam, C. Ohlen, J.J. Neefjes, P. Hoglund, M.T. Heemels, J. Bastin, T.N. Schumacher, A. Townsend, K. Karre, H.L. Ploegh, Empty MHC class I molecules come out in the cold, *Nature*, 346 (1990) 476-480.
- [24] V. Ortiz-Navarrete, G.J. Hammerling, Surface appearance and instability of empty H-2 class I molecules under physiological conditions, *Proc Natl Acad Sci U S A*, 88 (1991) 3594-3597.
- [25] L. Saveanu, O. Carroll, M. Weimershaus, P. Guermonprez, E. Firat, V. Lindo, F. Greer, J. Davoust, R. Kratzer, S.R. Keller, G. Niedermann, P. van Endert, IRAP identifies an endosomal compartment required for MHC class I cross-presentation, *Science*, 325 (2009) 213-217.
- [26] F. Zhang, W. Zhang, L. Liu, C.L. Fisher, D. Hui, S. Childs, K. Dorovini-Zis, V. Ling, Characterization of ABCB9, an ATP binding cassette protein associated with lysosomes, *J Biol Chem*, 275 (2000) 23287-23294.

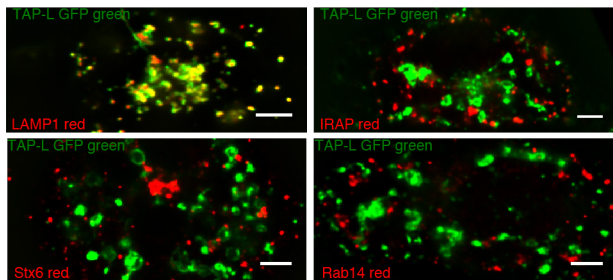
- [27] A. Burgevin, L. Saveanu, Y. Kim, E. Barilleau, M. Kotturi, A. Sette, P. van Endert, B. Peters, A detailed analysis of the murine TAP transporter substrate specificity, *PLoS One*, 3 (2008) e2402.
- [28] A. Lev, M.F. Princiotta, D. Zanker, K. Takeda, J.S. Gibbs, C. Kumagai, E. Waffarn, B.P. Dolan, A. Burgevin, P. Van Endert, W. Chen, J.R. Bennink, J.W. Yewdell, Compartmentalized MHC class I antigen processing enhances immunosurveillance by circumventing the law of mass action, *Proc Natl Acad Sci U S A*, 107 (2010) 6964-6969.
- [29] P.M. Van Endert, D. Riganelli, G. Greco, K. Fleischhauer, J. Sidney, A. Sette, J.-F. Bach, The peptide-binding motif for the human transporter associated with antigen processing, *J.Exp.Med.*, 182 (1995) 1883-1895.
- [30] M.A. Miller, A.P. Ganesan, N. Luckashenak, M. Mendonca, L.C. Eisenlohr, Endogenous antigen processing drives the primary CD4+ T cell response to influenza, *Nat Med*, 21 (2015) 1216-1222.
- [31] B. Chatterjee, A. Smed-Sorensen, L. Cohn, C. Chalouni, R. Vandlen, B.C. Lee, J. Widger, T. Keler, L. Delamarre, I. Mellman, Internalization and endosomal degradation of receptor-bound antigens regulate the efficiency of cross presentation by human dendritic cells, *Blood*, 120 (2012) 2011-2020.
- [32] G. Basha, G. Lizee, A.T. Reinicke, R.P. Seipp, K.D. Omilusik, W.A. Jefferies, MHC class I endosomal and lysosomal trafficking coincides with exogenous antigen loading in dendritic cells, *PLoS One*, 3 (2008) e3247.
- [33] G. Lizee, G. Basha, J. Tiong, J.P. Julien, M. Tian, K.E. Biron, W.A. Jefferies, Control of dendritic cell cross-presentation by the major histocompatibility complex class I cytoplasmic domain, *Nature immunology*, 4 (2003) 1065-1073.



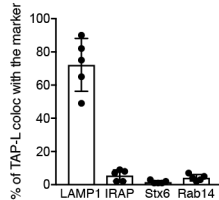


BMDCs	Geometric mean	
	AF6	B8.24.3
Control	22.4	17.8
WT 37°C	129	147
WT 26°C	154	160
TAP ^{-/-} 37°C	55.5	49
TAP ^{-/-} 26°C	62.3	91.6
TAP-L ^{-/-} 37°C	157	175
TAP-L ^{-/-} 26°C	191	226
Double KO 37°C	55.3	45.4
Double KO 26°C	62.5	104

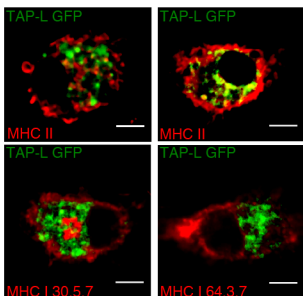
A



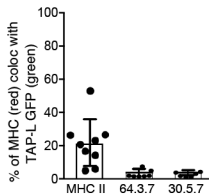
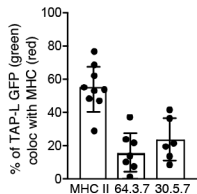
TAP-L GFP in BMDCs



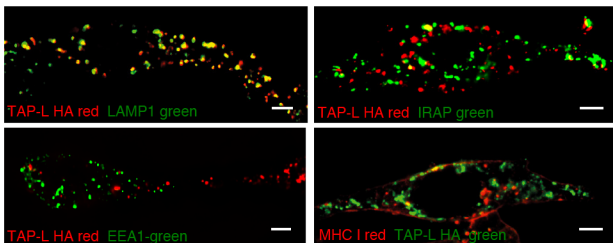
B



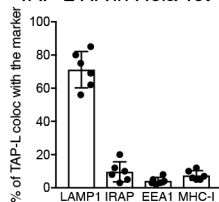
TAP-L GFP with MHC

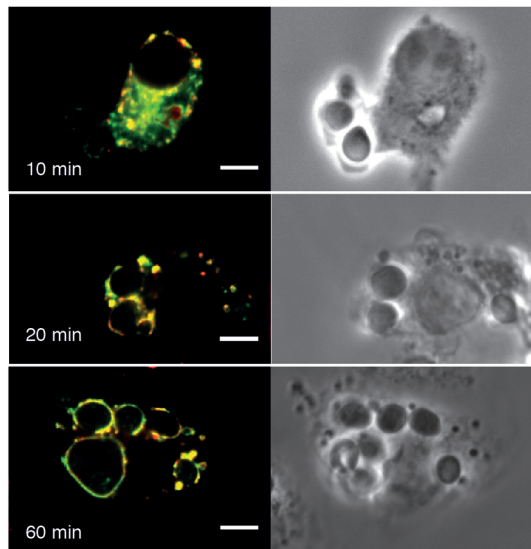
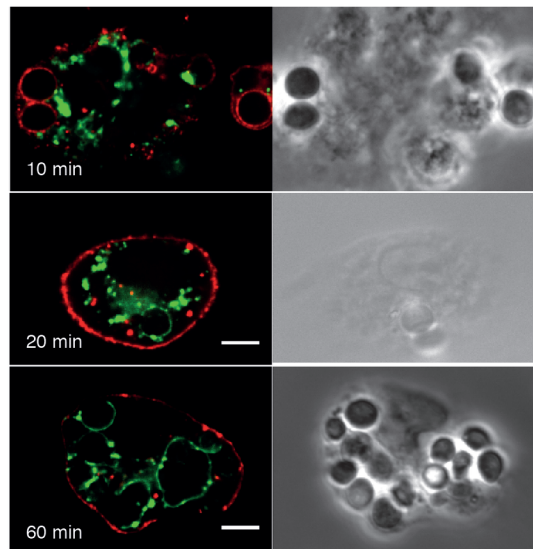
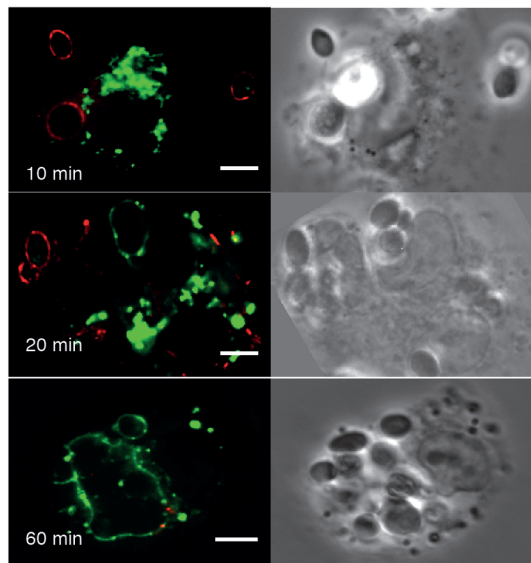
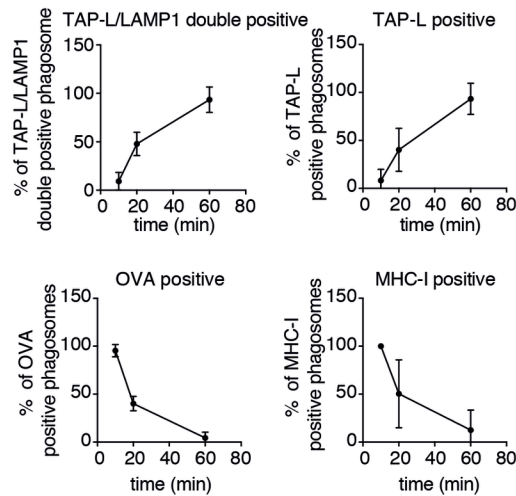


C

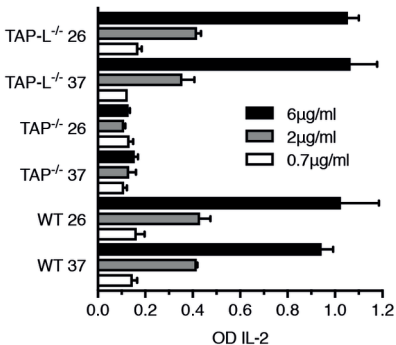


TAP-L HA in HeLa Tet-ON

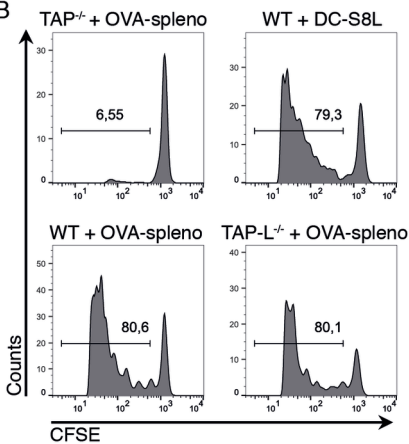


A TAP-L-GFP green LAMP1 red**C** TAP-L-GFP green MHC-I red**B** TAP-L-GFP green OVA red**D**

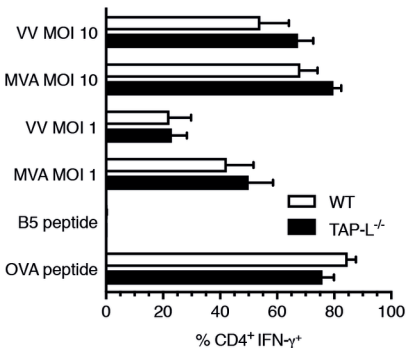
A

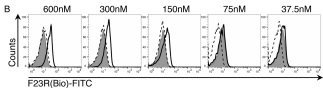
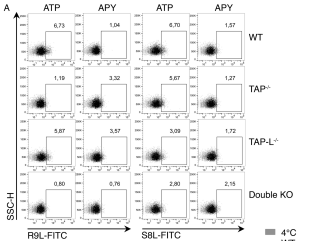


B



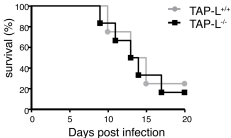
C





A

IAV infection 150 pfu/mice



B

IAV infection 300 pfu/mice

